Cell Stress and Chaperones (2017) 22:729–742
DOI 10.1007/s12192-017-0800-2

ORIGINAL PAPER

Hsp90 inhibitors radicicol and geldanamycin have opposing effects on *Leishmania* Aha1-dependent proliferation

Katharina Bartsch[1] · **Antje Hombach-Barrigah**[1] · **Joachim Clos**[1]

Received: 3 March 2017 / Revised: 4 April 2017 / Accepted: 11 April 2017 / Published online: 28 April 2017

Abstract Hsp90 and its co-chaperones are essential for the medically important parasite *Leishmania donovani*, facilitating life cycle control and intracellular survival. Activity of Hsp90 is regulated by co-chaperones of the Aha1 and P23 families. In this paper, we studied the expression of *L. donovani* Aha1 in two life cycle stages, its interaction with Hsp90 and the phenotype of Aha1 null mutants during the insect stage and inside infected macrophages. This study provides a detailed in vitro analysis of the function of Aha1 in *Leishmania* parasites and the first instance of a reverse genetic analysis of Aha1 in a protozoan parasite. While Aha1 is non-essential under standard growth conditions and at elevated temperature, Aha1 protects against ethanol stress. However, both overexpression and lack of Aha1 affected parasite growth in the presence of the Hsp90 inhibitors radicicol (RAD) and geldanamycin (GA). Under RAD pressure, P23 and Aha1 act in an antagonistic way. By contrast, expression levels of both co-chaperones have similar effects under GA treatment, indicating different inhibition mechanisms by the two compounds. Aha1 is also secreted in virulence-enhancing exosomes. This may explain why the loss of Aha1 reduces the infectivity of *L. donovani* in ex vivo mouse macrophages, indicating a role during the intracellular mammalian stage.

Keywords *Leishmania* · Aha1 · Hsp90 · Co-chaperone · Inhibitors · Exosomes

Introduction

Infections caused by protozoan parasites of the genus *Leishmania* are among the most important Neglected Tropical Diseases. They are poverty-related, and therapeutic options are limited and fraught with high costs and severe side effects. Leishmaniae are transmitted by several genera of Dipteran sandflies and undergo three stages to complete their life cycle. In the sandflies, leishmaniae proliferate as elongated, flagellated promastigotes, attached to the epithelium of the hindgut. Upon reaching high density, they undergo a change of their surface lipophosphoglycans and become more motile. These forms, metacyclic promastigotes, detach from the gut epithelium and can be inoculated into a mammal when the sandfly takes a blood meal. Inside the mammalian host, leishmaniae are phagocytised by antigen-presenting cells, chiefly macrophages, and undergo a morphological change towards an ovoid, aflagellated amastigote stage that survives and proliferates inside macrophages, destroying them and causing the various, species-specific immune pathologies. This differentiation process, from promastigote to amastigote, is essential for the parasite's survival and is triggered by the changes of temperature and milieu during transmission.

The intracellular amastigote stage can be mimicked in vitro, in axenic culture, by exposing promastigotes to mammalian tissue temperature (35–39 °C) and an acidified (pH 5–5.5) growth medium (Barak et al. 2005; Bates 1993, 1994; Zilberstein and Shapira 1994). The major chaperone, Hsp90, is crucial for this temperature-induced differentiation. Pharmacological inhibition of Hsp90 using antibiotics such as geldanamycin (GA) or radicicol (RAD) can induce

Electronic supplementary material The online version of this article (doi:10.1007/s12192-017-0800-2) contains supplementary material, which is available to authorized users.

✉ Joachim Clos
clos@bnitm.de

[1] Bernhard Nocht Institute for Tropical Medicine, Bernhard Nocht St. 74, 20359 Hamburg, Germany

promastigote-to-amastigote differentiation in vitro in the absence of a temperature or milieu change (Hombach et al. 2013; Wiesgigl and Clos 2001).

Hsp90 is known to serve as nucleus of a multi-subunit chaperoning complex, also known as the Hsp90 foldosome (Buchner 1999; Li et al. 2011; Wandinger et al. 2008). Known subunits include but are not limited to heat shock protein 70 (Hsp70) and heat shock protein 40 (Hsp40), so-called co-chaperones of which the best conserved is Stip1 (stress-inducible protein1, a.k.a. Sti1). Co-chaperones are responsible for foldosome assembly, client protein specificity and regulation of the chaperoning cycles. Since both Hsp90 and Hsp70 are energy-dependent chaperones with ATPase activity, regulation of activity targets the nucleotide-binding domain (NBD). The NBD of Hsp90, due to its particular structure, is also the target of GA and RAD which inhibit Hsp90 family chaperones exclusively.

Leishmania parasites have conserved most known co-chaperones (Johnson and Brown 2009). Several have already been studied using reverse genetics. Stip1, its proper phosphorylation state and its interaction with Hsp90 are essential for survival in both life cycle stages (Hombach et al. 2013; Morales et al. 2010). Another essential co-chaperone in *Leishmania* is the small glutamine-rich tetratricopeptide repeat protein (TPR) which together with Stip1 is part of the foldosome (Ommen et al. 2010). Deletion of the gene for cyclophilin 40 (Cyp40) causes a conditional phenotype, affecting morphology of late-stage promastigotes and severely impeding the ability of the parasite to survive inside macrophage host cells (Yau et al. 2014, 2016). Other putative co-chaperones are a HIP-like protein and another TPR domain-containing protein annotated as HOP-2 which both can be deleted without apparent loss of function phenotype (Ommen et al. 2009).

All of the above described co-chaperones are distinguished by TPR domains which are involved in co-chaperone-chaperone recognition. In addition to these TPR co-chaperones, two co-chaperones are involved in the regulation of Hsp90 ATPase activity—P23 and Aha1 (Rehn and Buchner 2015). Both act antagonistically, with P23 limiting ATPase activity and **A**ctivator of **H**sp90 **A**TPase (Aha1) promoting it. In higher eukaryotes, Aha1 consists of one N-terminal domain and one C-terminal domain, where the N-terminal domain interacts with the NBD of Hsp90. In human and in yeast, a second orthologue of Aha1 is present. The structure of Aha1 in lower eukaryotes differs; e.g. Aha1 in the protozoan parasites *Plasmodium falciparum* and *Toxoplasma gondii* is composed of two N-terminal domains and one C-terminal domain. The architecture of Aha1 in other protozoan parasites, e.g. *Giardia lamblia* and *Entamoeba histolytica*, is reduced to either of the two domains without losing ATPase activation activity (Rehn and Buchner 2015; Singh et al. 2014). The Aha1 gene is also conserved in the protozoan parasite *Leishmania* spp. A structural study of Aha1 in *Leishmania braziliensis*, the causative agent of mucocutaneous leishmaniasis, has already been published. Similar to human and yeast Aha1, the protein in *L. braziliensis* also comprises two domains (N-terminal and C-terminal domain) which stimulate the ATPase activity of Hsp90 in vitro (Seraphim et al. 2013). The putative antagonist of Aha1, P23, is encoded by two P23-like genes in the *Leishmania* genomes. The two P23 proteins exhibit similar structures and HSP90-binding properties (Batista et al. 2015) but have different functions. One gene was found to be essential for survival of *Leishmania* at temperature >30 °C and thus for survival inside mammalian macrophages, and it was therefore named heat shock protein 23 (Hsp23) (Hombach et al. 2014). The other, named P23, was dispensable under most in vitro cultivation conditions, but protects Hsp90 against GA and even more against RAD (Hombach et al. 2015). Null mutants of P23 are hypersensitive to both compounds, but overexpression does not increase tolerance.

In this paper, we study *L. donovani* Aha1 on a cellular and subcellular level. We show that Aha1 is expressed constitutively and interacts with Hsp90. We describe the first Aha1 deletion mutant in a protozoan parasite and observe that the protein is dispensable for growth under heat stress but required for ethanol tolerance. Interestingly, the deletion of Aha1 renders the cells sensitive to GA but not to RAD. Furthermore, Aha1 is involved in intracellular survival and is part of the *Leishmania* secretome.

Materials and methods

L. donovani culture

L. donovani 1SR (Rosenzweig et al. 2008) promastigote parasites were cultivated as described before (Krobitsch et al. 1998) in supplemented M199 at 25 °C. Electrotransfected parasites were cultivated in supplemented M199 with the appropriate selection antibiotics. For routine cell culture, parasites were allowed to grow to late logarithmic phase in order to maintain exponential growth. Cell density was measured using a CASY Cell Counter and Analyzer (Roche, Basel). The IC_{50} of ethanol, radicicol (Sigma-Aldrich, Munich) and geldanamycin (InvivoGen, Toulouse) was determined experimentally by dose-inhibition analysis.

Electrotransfection and selection

Electrotransfection was performed as previously described (Ommen and Clos 2010). Promastigote *L. donovani* were taken from mid-logarithmic culture, sedimented and washed twice in ice-cold phosphate-buffered saline (PBS) and once in electroporation buffer, and then resuspended at a density of 1×10^8 mL^{-1} in 0.4 mL of electroporation buffer (Kapler et al. 1990; Laban and Wirth 1989) with 2 μg of linearised DNA (homologous

recombination) or 50 μg circular DNA (episomal transfection). Electroporation was immediately carried out with the Gene Pulser apparatus (Bio-Rad, Munich) at 2.750 V cm^{-1}, 25 μF and 200 Ω with three pulses using a 4-mm electroporation cuvette. Cells were incubated on ice for 10 min and added to 10 mL of supplemented M199. After 24 h, the appropriate selection antibiotics, bleomycin (5 μg mL^{-1}, VWR, Darmstadt, Germany), puromycin (25 μg mL^{-1}, AppliChem, Darmstadt, Germany), G418 (50 μg mL^{-1}, Roth, Karlsruhe, Germany) or nourseothricin (150 μg mL^{-1}, WERNER BioAgents, Jena, Germany), were added.

For limiting dilution of promastigote parasites, 0.5 cells per well were seeded in multi-well plates in supplemented M199 with the appropriate selection antibiotics. Ten to 14 days after seeding, wells positive for cell growth were identified and the cells were transferred into supplemented M199 with antibiotics.

In vitro stage differentiation

L. donovani underwent an in vitro, axenic life cycle as described (Hombach et al. 2014a). Briefly, late logarithmic promastigotes (day 1) were subjected to a 37 °C temperature increase for 24 h before acidification of the medium (pH 5.5, day 2) and continued cultivation at 37 °C for promastigote-to-amastigote differentiation. Amastigotes (day 8) were cultivated at lowered temperature (25 °C) and raised pH (7.0) for amastigote-to-promastigote differentiation (days 9 and 10). Cell density measurements were performed with the CASY Cell Counter. Cell lysates of equal cell volume were subjected to sodium dodecyl sulphate polyacrylamide gel electrophoresis (SDS-PAGE) and Western blotting. Protein bands were quantified densitometrically using the ImageJ software 1.49v (Wayne Rasband, National Institutes of Health, MD, USA).

In vitro infection experiments

Mouse bone marrow-derived macrophages (BMMs) were differentiated from progenitor cells from the femurs and tibias of female C57BL/6 mice using Dulbecco's Modified Eagle Medium (DMEM) supplemented with 10% heat-inactivated FCS, 5% horse serum, 1× penicillin-streptomycin solution, 1× GlutaMAX supplement and 10–30% supernatant of LADMAC cells (Racoosin and Swanson 1989). After differentiation into macrophages, BMMs were harvested, washed and seeded into 12-well plates (TPP, Trasadingen, Switzerland) at a density of 2×10^5 cells per well. Macrophages were incubated for 48 h at 37 °C and 5% CO_2 to allow adhesion. The adherent macrophages were infected with stationary-phase promastigotes (Racoosin and Beverley 1997) at a multiplicity of infection of 10 parasites per macrophage. After 4 h of infection at 37 °C and 5% CO_2 in supplemented DMEM as described above, free parasites were washed off with PBS, and incubation was continued for another 44 h at 37 and 5% CO_2. At 4.5 and 48 h post infection, free and attached cells were pooled by sedimentation and lysed. Genomic DNA (gDNA) was isolated from the infected cells using the ISOLATE II Genomic DNA Kit (Bioline, Luckenwalde, Germany). Intracellular parasites were then quantified by semi-quantitative real-time PCR (qPCR) targeting host cell and parasite actin-coding genes with dually labelled probes and using total parasite and host gDNA as the templates (Bifeld et al. 2016). The relative parasite load was defined as the ratio of parasite actin DNA versus mouse actin DNA, with the value for *L. donovani* wild-type parasites set at 100%.

Construction and preparation of recombinant DNA

Approximately 1000 bp of 5′ non-coding (5′ NC) DNA and 3′ non-coding (3′ NC) DNA of the Aha1 gene (LinJ.18.0210) were amplified enzymatically from genomic *L. donovani* DNA with primers that created single *Kpn*I and *Bam*HI sites between 5′ NC and 3′ NC. Two *Swa*I sites flank the constructs. The 5′ NC and 3′ NC amplificates were ligated into pUC19 (Yanisch-Perron et al. 1985) using the In-Fusion HD Cloning Kit (Takara Bio Europe SAS, Saint-Germain-en-Laye, France). The resulting pUC19-Aha1-5′-3′NC was cut with *Kpn*I and *Bam*HI. Bleomycin and puromycin resistance genes were ligated between the Aha1 flanking sequences in pUC19-Aha1-5′-3′NC to yield pUC19-Aha1-5′bleo3′ and pUC19-Aha1-5′puro3′ (Fig. S2A). The plasmids were amplified in *E. coli*, purified by caesium chloride density gradient ultracentrifugation (Sambrook and Russell 2001) and linearised with *Swa*I (Fig. S2B). The fragments containing the recombination cassette were separated by agarose gel electrophoresis and purified using the NucleoSpin Gel and PCR Clean-Up Kit (Macherey-Nagel, Düren, Germany).

To create pCL2N-Aha1 (LinJ.18.0210), coding sequences were amplified introducing *Kpn*I and *Bam*HI sites respectively to the 5′ and 3′ ends, and fused into pCL2N (Schäfer et al. 2014) between the matching restriction sites.

To create pCL2S-Aha1 or pCL2N-P23 (LinJ.35.4540), coding sequences were excised from pCL2N-Aha1 or pCLS-P23 (Hombach et al. 2015) and then fused into pCL2S (Hombach et al. 2014a) or pCL2N respectively.

To create pCLN-3HA::Aha1, Aha1-coding sequences were amplified introducing *Nde*I and *Bam*HI sites respectively to the 5′ and 3′ ends, followed by ligation into pCLN-3HA (Hombach et al. 2013) between the *Nde*I and *Bam*HI sites.

The plasmids pTL.v6-Hsp90rr and pCLN-3HA::Hsp90 (Hombach et al. 2013) and the generation of *L. donovani* $P23^{-/-}$ null mutants (Hombach et al. 2015) were described before.

Verification of null mutants

Mutant genotypes were verified by PCR analysis of gDNA. The preparation of gDNA was carried out using the Gentra

Puregene Tissue Kit (Qiagen, Hilden, Germany) following the manufacturer's instructions.

The Aha1 gene replacement was verified by PCR using the Aha1-specific primers Aha1-ORF-fwd (ATGGCCAA GGTCGGTGAG) and Aha1-ORF-rev (TCACATGT ACTCGAGCGAG). The quality of the isolated gDNA of the Aha1 gene replacement mutants was verified by PCR using primers for the Hsp23 gene, i.e. Hsp23-fwd (ATGTCCACCAGCGGCCCA) and Hsp23-rev (CTCGAGGAGGACACGTGA). To verify the correct integration of the selection marker genes in the Aha 1 gene locus, control PCRs were performed using primers Aha1-5′-flank (TTATTATTAAGACCGTGGTGAG), Aha1-3′-flank (CACACGCACTCGTTACGTGC), BleoR-5′rev (GGAACGGCACTGGTCAAC), BleoR-3′fwd (GCAACTGCGTGCACTTCG), PuroAC-5′rev (GTGGGCTTGTACTCGGTC) and PuroAC-3′fwd (GGTGCATGACCCGCAAGC).

Expression profiling

For the expression profiling, a semi-quantitative real-time RT-PCR was performed as described (Choudhury et al. 2008). The Aha1-coding region primers were Aha1-fwd (CACATGTCAGGATAACGACGC) and Aha1-rev (GATACTCGGTGAAGAGGGCAT) while the primers bracketing the border between Aha1-coding sequence (CDS) and 3′ NC of Aha1 were Aha1-NC-fwd (GGGCAAAC TTCTTCGAGGCTA) and Aha1-NC-rev (GACTTCGT TCTTCCTCCTCCG). Aha1 mRNA abundance was normalised against the *Leishmania* actin signal.

Recombinant protein expression in *E. coli* and protein purification

The expression of Aha1 was performed as previously described (Schlüter et al. 2000) using the expression vector pJC57 with the Aha1 CDS integrated. The (His_{10})::Aha1 protein was purified by metal chelate affinity chromatography as described (Clos and Brandau 1994).

Immunisation and antibody preparation

The purified Aha1 proteins were used to immunise laying hens. Anti-Aha1 IgY was isolated from the egg yolk as described (Hübel et al. 1995). Isolated anti-Aha1 IgY were tested against lysates from *L. major* 5ASKH, *L. donovani* 1SR, *Trypanosoma cruzi* Y, *T. cruzi* Tulahuen and recombinant (His_{10})::Aha1. Immunisation of laying hens was performed in accordance with §8a, German Animal Protection Law, and registered with the Amt für Gesundheitlichen Verbraucherschutz, Behörde für Umwelt und Gesundheit, Freie und Hansestadt Hamburg.

SDS-PAGE and Western blot analysis

Production of *L. donovani* cell lysates, discontinuous SDS-PAGE and Western blotting was performed according to standard protocols (Brandau et al. 1995) using FluoroTrans PVDF membranes (VWR). Membranes were blocked with blocking solution (5% milk powder in Tris-buffered saline (TBS), 0.1% Tween 20), probed with chicken anti-Aha1 (1:500 in blocking solution), chicken anti-Hsp90 (1:1000 in blocking solution), chicken anti-Cpn60.2 (1:1000 in blocking solution) or mouse anti-HslU1 (1:1000 in blocking solution) before incubation with anti-chicken IgG-alkaline phosphatase (1:5000 in blocking solution, Dianova, Hamburg, Germany) or anti-mouse IgG-alkaline phosphatase (1:1000 in blocking solution, Dianova). Blots were developed using nitro blue tetrazolium chloride (Roth) and 5-bromo-4-chloro-3-indolyl phosphate (Biomol, Hamburg).

Cell fractionation

The intracellular localisation of Aha1 in *L. donovani* 1SR wild-type cells was determined as previously described by a two-step digitonin lysis (Rey-Ladino et al. 1997; Schlüter et al. 2000; Tejera Nevado et al. 2016). The cytosolic, intermediate and mitochondrial fractions were separated by SDS-PAGE and subjected to Western blot.

Immune precipitation

L. donovani wild-type parasites or wild-type cells transfected with pCLN-3HA::Hsp90 or pCLN-3HA::Aha1 transgenes, carrying three tandem, N′ terminal haemagglutinin (HA) epitopes, were taken from a late logarithmic culture (1×10^8), sedimented and washed twice in ice-cold PBS. For the cross-linking of protein complexes, the cells were treated with 0.5 mM dithiobis(succinimidyl propionate) (DSP, Pierce) and incubated at room temperature for 30 min. Cross-linking was quenched by the addition of 25 mM Tris-HCl (pH 7.5) and incubation for 15 min at room temperature. The cross-linked samples were sedimented, lysed with cell lysis buffer (100 mM Tris-HCl [pH 7.5], 150 mM NaCl, 0.5 mM EDTA, 2% Triton X-100, 1 mM phenyl methane sulphonyl fluoride (PMSF), 0.5 mM 1,10-phenanthroline) for 1 h on ice and sedimented (20,000×*g*, 4 °C, 10 min). The supernatant was adjusted to a volume of 450 μL with wash buffer (1× TBS, 0.05% Tween 20, 1 mM PMSF, 0.5 mM 1,10-phenanthroline), and 50 μL of cell lysate was saved for analysis ('input' fraction). The cell lysates were mixed with 50 μL of pre-washed anti-HA magnetic beads (Thermo Fisher Scientific, Waltham, MA, USA) and incubated by end-over-end mixing at room temperature for 2 h. The washing and elution of

the HA-tagged proteins (with sample buffer) was performed following the manufacturer's instructions. The input and 'bound' fraction samples were subjected to SDS-PAGE and Western blot analysis.

Secretome analysis

Proteins secreted by *L. donovani* 1SR wild-type promastigotes were isolated as described (Tejera Nevado et al. 2016; Twu et al. 2013). The concentrated secretome was stored at −80 °C.

Trypsin digestion

After isolation of the *L. donovani* secretome, the concentrated secretome was subjected to trypsin digestion to verify intact vesicles (Bifeld et al. 2015; Silverman et al. 2010a; Tejera Nevado et al. 2016). In brief, the isolated concentrated secretome was resuspended either in 20 mM Tris-HCl (pH 7.4) with 40 μg mL^{-1} trypsin (Promega, Mannheim, Germany), in 20 mM Tris-HCl (pH 7.4) with 40 μg mL^{-1} trypsin and 0.1% Triton X-100 or in 20 mM Tris-HCl (pH 7.4) alone at 37 °C for 1 h. The trypsin digestion was inactivated by the addition of 22 mM PMSF. The samples were mixed for 10 s; four volumes of ice-cold acetone was added for precipitation and incubated at −20 °C for 2 h. The samples were sedimented (16,000×*g*, 4 °C, 10 min) and the pellet air-dried. The secretome samples were subjected to SDS-PAGE followed by Western blot analysis.

Immunofluorescence microscopy

For the determination of parasites' cell body length and flagellum length, promastigote parasites in logarithmic phase (1×10^7) were sedimented, washed twice in ice-cold PBS and resuspended in 1 mL PBS. Approximately 2×10^5 cells were applied to microscopic slides and air-dried. Cells were fixed by incubation in ice-cold methanol for 2 min and again air-dried. The slides were washed (0.1% Triton X-100 in PBS) to remove non-adherent cells, incubated in permeabilisation solution (0.1% Triton X-100, 50 mM NH_4Cl in PBS) for 20 min, followed by incubation in blocking solution (2% bovine serum albumin, 0.1% Triton X-100 in PBS) for 1 h. Then, the slides were incubated with mouse anti-α-tubulin (1:4000 in blocking solution, Sigma-Aldrich) for 1 h. Cells were washed thrice and incubated with anti-mouse Alexa Fluor 594 (1:500 in blocking solution, Thermo Fisher Scientific) and DAPI (1:50 in blocking solution, Sigma-Aldrich) for 1 h. The slides were washed thrice before Mowiol and coverslips were applied, and the slides were left to dry for 24 h at 4 °C. The analysis of the cell body length and flagellum length was performed using an EVOS FL Auto epifluorescence microscope (Thermo Fisher Scientific) and the measuring tool of the EVOS FL Auto software.

In silico procedures

Numerical data were analysed using Prism software 5.0a (GraphPad Inc., La Jolla CA, USA). DNA and protein sequence analysis was carried out using MacVector software 15.1.4 (MacVector Inc., Apex, NC, USA). Optimisation of greyscale and colour images was performed using Adobe Photoshop CS3 software 10.0.1 (Adobe Systems Inc., San Jose, CA, USA). Figures were assembled using Intaglio software 3.9.4 (Purgatory Design, Durango, CO, USA). Significances were calculated using the Mann-Whitney *U* test (Mann and Whitney 1947) or the paired Student's *t* test (Student 1908).

Results

Expression of Aha1 in *Leishmania*

Some, but not all, molecular chaperones of *Leishmania* spp. show a stage-dependent expression pattern, i.e. elevated expression in amastigotes (Clos and Hombach 2015). To determine expression rates for Aha1 during an axenic life cycle, we produced anti-Aha1 IgY in immunised chickens as detailed in the "Materials and methods" section. The antibodies were tested in Western blots against lysates from two *Leishmania* species and two *T. cruzi* strains and against recombinant Aha1 from *E. coli*. Bands corresponding to a molecular mass of ~42 kD are detected in lysates from *L. major* and *L. donovani* (Fig. S1), but not in the *T. cruzi* lysates reflecting the poor sequence conservation (56%) between the leishmaniae and the trypanosomes. The slightly larger recombinant Aha1 (~44 kD) was included as positive control.

We used the Aha1-specific antibodies to probe lysates from *L. donovani* undergoing an axenic stage conversion cycle (Fig. 1a). Logarithmically growing (25 °C) promastigotes (day 1) were subjected to a temperature shift to 37 °C (day 2) and subsequent acidification of the medium (pH 5.5, days 3–8) during which axenic amastigotes formed (not shown). Lowering the temperature to 25 °C and increasing the pH to 7 (days 9–10) induced a reversal back to the promastigote stage (not shown). During this axenic-stage conversion cycle, Aha1 steady-state levels showed no detectable changes relative to the total amount of protein (Fig. 1b, c). We conclude that Aha1 in *L. donovani* is a constitutively expressed protein, in keeping with earlier work performed with *Leishmania* (*Viannia*) spp. and *L. infantum* (Seraphim et al. 2013).

Aha1 binds to HSP90

Aha1, as implied by its name, typically interacts with Hsp90. This was confirmed for *L. braziliensis* by isothermal titration calorimetry (ITC) with recombinant Hsp90 and Aha1

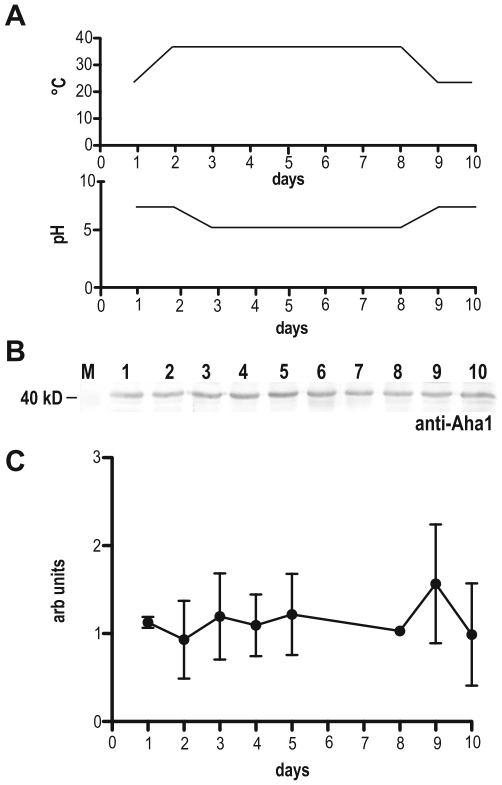

Fig. 1 Expression kinetics for Aha1 in *L. donovani*. To monitor the expression of Aha1 during an axenic life cycle, a promastigote-to-amastigote conversion was performed. **a** The temperature and pH profiles are shown. **b** Aha1 protein abundance (days 1–10) was analysed by Western blot. Cell lysates were separated by SDS-PAGE, subjected to Western blot and probed with chicken anti-Aha1. As a loading control, a replica gel was stained with Coomassie Brilliant Blue (not shown). The position of the 40-kD-size marker is shown on the *left*. **c** Aha1 protein abundance (arbitrary units) was quantified by Western blot and densitometry and plotted against time

(Seraphim et al. 2013). To test for a physical interaction between Hsp90 and Aha1, we performed a series of co-immune precipitations using overexpressed Hsp90 or Aha1 that were tagged with a triplicate 12CA5 epitope of human influenza virus haemagglutinin protein (3HA tag). The 3HA::Hsp90 and 3HA::Aha1 transgenes were expressed episomally in *L. donovani*. The recombinant parasites and a wild-type control were treated with the cross-linking reagent DSP and subjected to lysis. Lysates were then mixed with anti-HA magnetic beads in a magnetic field. The pulled-down material as well as the unselected lysates were then examined by SDS-PAGE and Western blotting, using anti-Hsp90 or anti-Aha1 antibodies (Fig. 2). The unselected fractions (input) show endogenously coded and overexpressed, tagged proteins (left panel). Immune precipitation of wild-type lysates does not generate signals with either antibodies. A pull-down using 3HA::Hsp90 shows the double band with anti-Hsp90 described before (Hombach et al. 2013), owing to the dimeric structure of Hsp90 complexes, but no signal with anti-Aha1. Conversely, a pull-down using 3HA::Aha1 produces a band

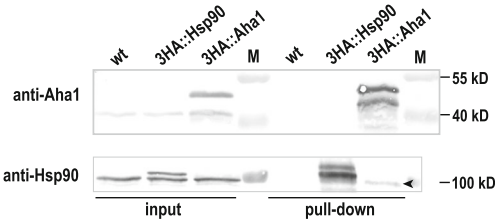

Fig. 2 Aha1 interacts with Hsp90. *L. donovani* wild-type parasites or wild-type cells transfected with 3HA::Hsp90 or 3HA::Aha1 transgenes were treated with 0.5 mM DSP followed by an anti-HA magnetic bead co-immune precipitation, SDS-PAGE and chicken anti-Aha1 or anti-Hsp90 Western blot. The *arrowhead* points at a Hsp90-specific band. Positions of size markers [kD] are shown in the *middle* and on the *right*

that is detected by the anti-Hsp90 antibodies (arrowhead). We conclude that, while 3HA-tagged Hsp90 cannot interact with Aha1, the tagged co-chaperone can indeed bind to the wild-type Hsp90, confirming a physical interaction between both proteins.

Aha1 is a cytosolic protein

We next determined the intracellular localisation of Aha1 in *Leishmania* promastigote cells. Being an early eukaryote organism, the leishmaniae possess two DNA-containing cell organelles, the nucleus and the kinetoplast, the latter being a part of the single, tubular mitochondrium and a hallmark of the order Trypanosomatida. Using a digitonin-based fractionation scheme (Schlüter et al. 2000), we separated cell lysates of *L. donovani* into cytosolic, intermediate and organelle (mitochondrial) fractions which were then analysed by SDS-PAGE and Western blot. The majority of Aha1 protein is found with the cytosolic fraction (Fig. 3a), mirroring the results for the known, cytosolic chaperone Hsp90 (Fig. 3b). Cpn60.2, a known mitochondrial protein (Schlüter et al. 2000; Zamora-Veyl et al. 2005), is detected in the mitochondrial fraction (Fig. 3c). Staining of a replica gel with Coomassie Brilliant Blue (Fig. 3d) verifies equal loading. In keeping with its proposed interaction with Hsp90, Aha1 too is a cytosolic protein.

Aha1$^{-/-}$ null mutants are viable

To further assess the role of Aha1 in *L. donovani*, we performed a double-allele gene replacement in two, sequential homologous recombination steps using bleomycin and puromycin resistance marker genes. Viable, double resistant parasites could be selected under the antibiotics and were cloned by limiting dilution. Ten individual clones were raised, and their genomic DNAs were subjected to PCR using gene-specific markers. Of the 10 clones, 10 were negative for Aha1-coding DNA. We also verified the correct integration of selection marker genes in place of *Aha1* (data not shown).

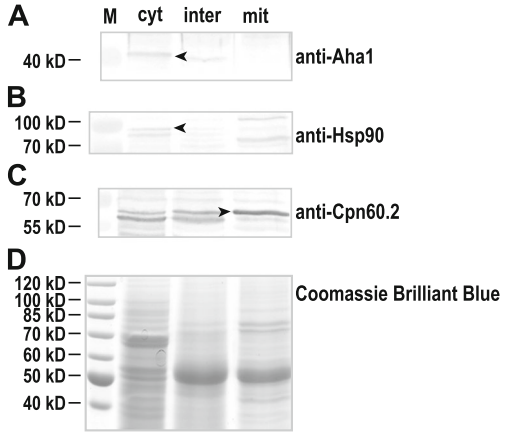

Fig. 3 Distribution of *L. donovani* Aha1 in cell fractions. *L. donovani* wild-type parasites were separated into the cytosolic (cyt), intermediate (inter) and mitochondrial (mit) fractions using a two-step digitonin lysis. The fractions were separated by SDS-PAGE, subjected to Western blot and probed with chicken anti-Aha1 (**a**), anti-Hsp90 (**b**) and anti-Cpn60.2 (**c**). As a loading control, a replica gel was stained with Coomassie Brilliant Blue (**d**). The *arrowheads* point at Aha1-, Hsp90- and Cpn60.2-specific bands. Positions of size markers [kD] are shown on the *left*

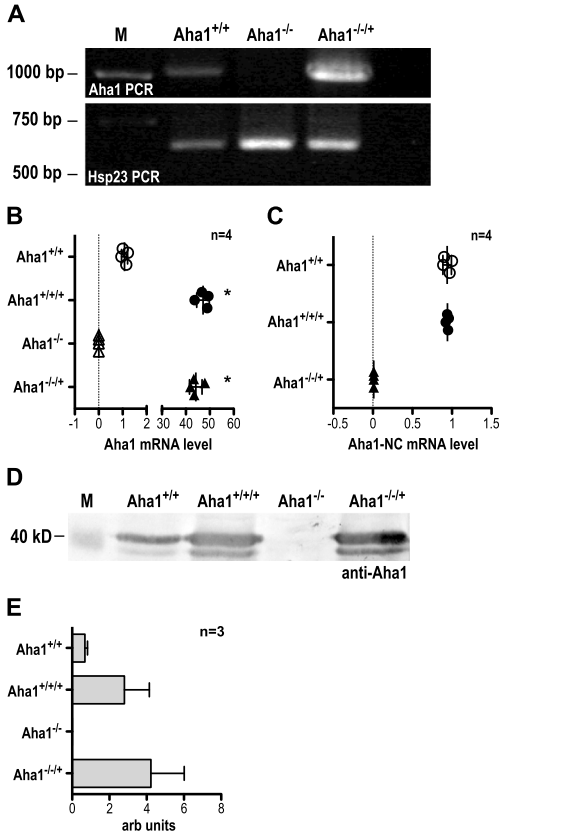

Fig. 4 Verification of *L. donovani* Aha1$^{-/-}$ null mutants and control strains. **a** The gDNAs from *L. donovani* strains Aha1$^{+/+}$ (wild type), Aha1$^{-/-}$ and Aha1$^{-/-/+}$ were used as templates for an Aha1 gene-specific PCR (*upper panel*). The same gDNAs were also used as templates for amplification of Hsp23-coding DNA (*bottom panel*) to ascertain the quality of the gDNAs. **b** Aha1 mRNA levels (arbitrary units) were quantified by RT-qPCR for Aha1$^{+/+}$, Aha1$^{+/+/+}$, Aha1$^{-/-}$ and Aha1$^{-/-/+}$ using primers against the coding region; $n = 4$; $*p \leq 0.05$ (Mann-Whitney *U* test). **c** Another RT-qPCR from the same samples was performed targeting either side of the border between Aha1 CDS and 3′ NC; $n = 4$. **d** Lysates from *L. donovani* strains Aha1$^{+/+}$, Aha1$^{-/-}$ and Aha1$^{-/-/+}$ were separated by SDS-PAGE, subjected to Western blot and probed with chicken anti-Aha1. A replica gel was stained with Coomassie Brilliant Blue as loading control (not shown). The position of the 40-kD-size marker is shown on the *left*; $n = 3$. **e.** Aha1 protein abundance (arbitrary units) was quantified by Western blot and densitometric analysis

Also, *L. donovani* Aha1$^{-/+}$ obtained after the first allele gene replacement using bleomycin selection were stably transfected with the pCL2N-Aha1 expression plasmid. After selection under G418, the resulting population was subjected to second-round gene replacement using puromycin selection. The triple selected parasites were cloned by limiting dilution plating. Correct integration of selection marker genes in place of *Aha1* was verified (not shown). Wild-type *L. donovani* were also stably transfected with the pCL2N-Aha1 plasmid to yield an overexpression (Aha1$^{+/+/+}$) strain.

Genomic DNA obtained from wild-type *L. donovani*, a supposed Aha1$^{-/-}$ null mutant clone (#2), and an Aha1$^{-/-/+}$ add-back clone were first subjected to PCR using Aha1-specific primers. As shown in Fig. 4a (upper panel), the signals for wild-type (Aha1$^{+/+}$) and add-back (Aha1$^{-/-/+}$) cells are positive, with a relative increase in the add-back sample. The double-allele gene replacement mutant (Aha1$^{-/-}$) is negative for Aha1 DNA. This is not due to quantitative or qualitative differences in the isolated gDNAs since Hsp23 DNA (Hombach et al. 2014) could be amplified from all gDNA preparations (Fig. 4a, lower panel).

Next, we quantified Aha1-specific RNA from wild-type *L. donovani* (Aha1$^{+/+}$), from Aha1 overexpressing cells with wild-type background (Aha1$^{+/+/+}$), from the null mutant clone 2 (Aha1$^{-/-}$) and from Aha1 overexpressing cells with null mutant background (add-back, Aha1$^{-/-/+}$). We used semi-quantitative real-time RT-PCR with primers against the Aha1-coding region. The data were normalised against actin complementary DNA (cDNA)-specific qPCR, and cDNA from the wild type was assigned the value ‘1’ (Fig. 4b). On the average of four samples, 47- and 44-fold increases were observed for Aha1$^{+/+/+}$ and Aha1$^{-/-/+}$, respectively, reflecting episomal expression from multiple gene copies. No amplification of Aha1 cDNA could be observed with template cDNA obtained from any of the Aha1$^{-/-}$ samples, corroborating the genomic DNA analysis in Fig. 4a.

To determine the source of Aha1 RNA in the Aha1$^{-/-/+}$ parasites, cDNA derived from wild-type *L. donovani* (Aha1$^{+/+}$), from Aha1 overexpressing cells with wild-type background (Aha1$^{+/+/+}$) and from Aha1 overexpressing cells with null mutant background (add-back, Aha1$^{-/-/+}$) were amplified using primers straddling the border between the Aha1-coding region and the 3′ non-coding region of Aha1. Since the

expression plasmid pCL2N-Aha1 uses the *L. donovani* LPG1 3′ non-coding region, cDNA derived from the episome-coded RNA cannot give rise to PCR products. Figure 4c shows the result. While wild-type ($Aha1^{+/+}$) and overexpressing parasites ($Aha1^{+/+/+}$) give equivalent results, the $Aha1^{-/-/+}$ cells produce no endogenously coded Aha1 RNA. Conversely, this means that all Aha1 RNA in the add-back clone is transgene-coded.

Lastly, we quantified Aha1 protein in wild-type *L. donovani* ($Aha1^{+/+}$), Aha1 overexpressing cells with wild-type background ($Aha1^{+/+/+}$), the null mutant clone 2 ($Aha1^{-/-}$) and Aha1 overexpressing cells with null mutant background clone 5 ($Aha1^{-/-/+}$) using Western blot analysis. Figure 4d shows that Aha1 levels increase moderately in transgene-carrying strains ($Aha1^{+/+/+}$ and $Aha1^{-/-/+}$) compared with the wild type. The $Aha1^{-/-}$ null mutant, by contrast, shows no signal for Aha1 protein at all, conclusively confirming $Aha1^{-/-}$ clone 2 as null mutant. The Western blots were quantified (Fig. 4e) densitometrically using a Coomassie Brilliant Blue-stained replicate SDS-PAGE (not shown) as loading control. The Western blot data also suggest that the >40-fold increase of Aha1 RNA does not translate into equally increased protein levels.

Growth phenotype of $Aha1^{-/-}$ null mutants

With the genotype of the null mutant and overexpressing parasites established, we first tested the growth of promastigote cells. Morphologically, the $Aha1^{-/-}$ null mutant showed a shortening of the flagellum compared with the wild type, while overexpression correlated weakly with increased flagellum length (Fig. S3B). This may be due to wild-type and Aha1 overexpression cells reaching higher cell density at the time point. Cell body length was unaffected (Fig. S3A).

Under standard growth conditions, i.e. 25 °C and pH 7.0, the Aha1 null mutant shows marginally slower growth (Fig. 5a), while the overexpressing parasites are indistinguishable from the wild type. At higher temperature (37 °C, pH 7.0), growth enters an early plateau for all strains (Fig. 5b), but again, $Aha1^{-/-}$ shows slightly but significantly ($p < 0.05$) lower cell counts. In acidic milieu (25 °C, pH 5.5), growth is slower, but $Aha1^{-/-}$ is lagging slightly behind the other strains (Fig. 5c). Challenge with ethanol at IC_{50} causes a 30% reduction of growth for the $Aha1^{-/-}$ null mutant. Conversely, the two Aha1 overexpressing strains, $Aha1^{+/+/+}$ and $Aha1^{-/-/+}$, grow faster than the wild type (Fig. 5d). The results strongly indicate a protective role for Aha1 under ethanol stress.

Aha1 enhances Hsp90 inhibition by radicicol, but not by geldanamycin

Aha1 has been described as being antagonistic to the co-chaperone P23 (Rehn and Buchner 2015). Earlier work has implicated *Leishmania* P23 in the resistance to the Hsp90 inhibitors RAD and GA (Hombach et al. 2015). We therefore compared $Aha1^{+/+/+}$, $Aha1^{-/-}$ and $Aha1^{-/-/+}$ under RAD (IC_{50} = 20–80 nM) challenge, using wild type ($Aha1^{+/+}$) and a strain expressing the radicicol-resistant Hsp90rr (Hombach et al. 2013) as controls. We also tested a P23-overexpressing strain ($P23^{+/+/+}$), the $P23^{-/-}$ null mutant and a dual $Aha1^{+/+/+}$/$P23^{+/+/+}$ overexpression strain.

As shown in Fig. 6a, Hsp90rr expression gives a slight advantage over wild-type parasites at IC_{50}. The $Aha1^{-/-}$ null mutant shows the same growth as the wild type, arguing against a role of Aha1 in protection against RAD. Surprisingly, Aha1-overexpressing parasites ($Aha1^{+/+/+}$ and $Aha1^{-/-/+}$) incur a significant exacerbation of the RAD-mediated growth inhibition. This effect is comparable to the severe growth inhibition observed for the $P23^{-/-}$ null mutant (Fig. 6a) described before (Hombach et al. 2015). The $P23^{+/+/+}$-overexpressing strain behaves like the wild type. However, combining overexpression of Aha1 and P23 causes an intermediate effect, reducing growth to ~50% of the wild type. The results indicate that Aha1 overexpression renders *L. donovani* more sensitive to RAD-mediated inhibition of Hsp90, thus acting in an antagonistic manner to the P23 co-chaperone.

Performing the equivalent experiment using GA (IC_{50} = 150–200 nM) as Hsp90 inhibitor yielded diametrically opposing results for the Aha1 mutants (Fig. 6b). Again, Hsp90rr protects against GA. However, overexpression of Aha1 ($Aha1^{+/+/+}$ and $Aha1^{-/-/+}$) has no additional effect on the growth compared with the wild type, while the $Aha1^{-/-}$ null mutant shows increased GA sensitivity. P23 overexpression has a slightly detrimental effect while the P23 null mutant is strongly hypersensitive to GA. The combined overexpression of Aha1 and P23 has a distinctly protective effect.

In summary, the results show that the Hsp90 inhibitors RAD and GA are differently affected by changes in the intracellular Aha1 concentration, perhaps reflecting different modes of action of the two Hsp90 inhibitors.

Loss of Aha1 reduces intracellular survival

Leishmania spp. are pathogens that chiefly infect and destroy the macrophages of the skin and the viscera, thereby causing various immune pathologies. Therefore, we tested the ability of the $Aha1^{-/-}$ null mutant to infect ex vivo mouse macrophages and compared it to that of wild-type and Aha1-overexpressing parasites. Mouse bone marrow-derived macrophages were seeded into multi-well plates and allowed to adhere, followed by addition of stationary growth phase promastigotes. After 4 h of exposure, free parasites were washed off. A first group of samples was taken for analysis to determine the infection rate while a second group of samples was incubated for a further 44 h to assess intracellular survival. Genomic DNA was then isolated from all samples for a PCR-based quantification of parasite load (Bifeld et al. 2016).

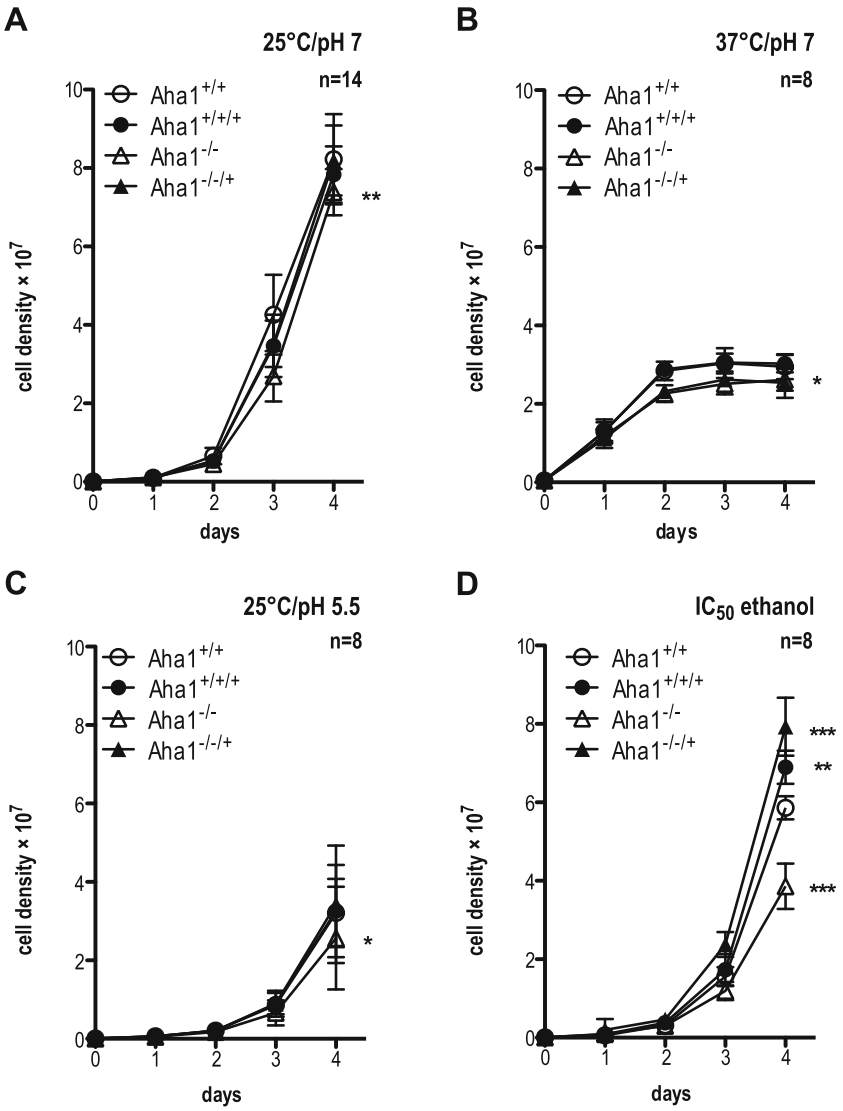

Fig. 5 Proliferation of Aha1$^{-/-}$ null mutants and control strains under stress. *L. donovani* cells (1×10^5 mL^{-1}) were seeded into 10 mL of supplemented M199 and grown for 4 days. The *y-axis* shows the cell density ($\times 10^7$). Parasites were grown at 25 °C and pH 7.0 ($n = 14$) (**a**), 37 °C and pH 7.0 (**b**) and 25 °C and pH 5.5 (**c**). Additional cultures were grown as in **a** with the addition of 2% ethanol (=IC_{50}) (**d**). $n = 8$; $^*p \le 0.05$; $^{**}p \le 0.01$; $^{***}p \le 0.001$ (paired Student's *t* test)

The initial infection rates of wild-type and mutant parasites can vary significantly (Fig. 7a). In particular, overexpression of Aha1 tends to increase uptake of the parasites by the macrophages while the null mutant is not affected. Forty-eight hours after infection, however, the null mutants show a significant ($p < 0.001$, $n = 18$), ~20% reduction of parasite load in the macrophages (Fig. 7b). This indicates a role for Aha1 during the intracellular amastigote stage.

Aha1 is secreted via vesicular export

A large part of the proteins secreted by *Leishmania* spp. is exported via exosome-like vesicles. This includes several proteins associated with virulence (Bifeld et al. 2015; Silverman et al. 2010a; Yau et al. 2016). Indeed, the *L. donovani* exosome fraction modulates the host immune response favourably for the parasite (Silverman et al. 2010b). Given the proven impact of Aha1 during the in vitro infection of macrophages (Fig. 7b), we decided to track Aha1 in the *L. donovani* secretome. For this, *L. donovani* was incubated for 2 h at 25 °C in PBS with 5% sucrose. The supernatant was sterile filtered, supplemented with peptidase inhibitor 1,10-phenanthroline and concentrated. After acetone precipitation of proteins, the pellets were then aliquoted and digested with trypsin or a combination of trypsin and Triton X-100 to disrupt membraneous vesicles. A third aliquot was left untreated. As shown in Fig. 8, Hsp90, a known exosomal protein, shows the expected results: it is detectable in the untreated sample and in the trypsin-only sample. The combination of membrane-disrupting Triton X-100 and trypsin caused degradation of Hsp90, confirming its intravesicular localisation (upper panel). The same pattern was observed for Aha1 (lower panel), confirming that it is part of the exosomal payload of *Leishmania*, possibly exerting its survival-enhancing effects in the host cell. The control using the anti-HslU1 antibody was

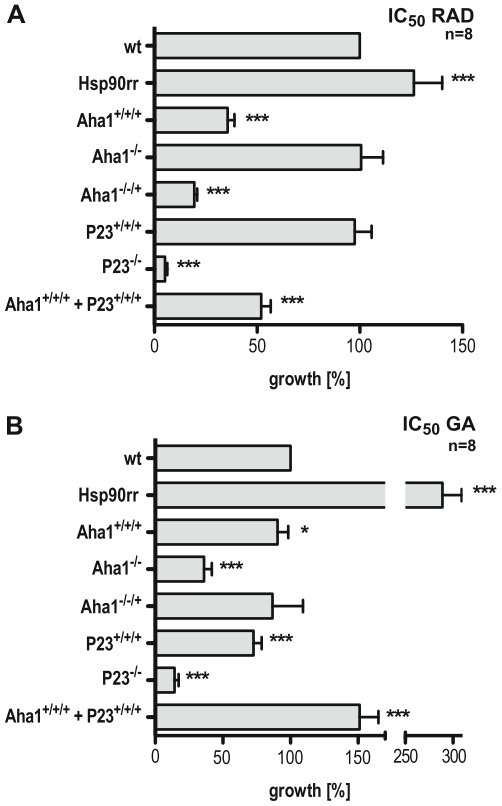

Fig. 6 Effects of Hsp90 inhibitors on the cell proliferation. *L. donovani* cells of various genetic background as indicated were seeded into 10 mL of supplemented M199 (1×10^5 mL^{-1}) and grown for 4 days at 25 °C and pH 7.0 with the addition of radicicol (**a**) or geldanamycin (**b**) at their IC_{50}. Mutant cell density on day 4 was normalised as percentage of wild-type cell density. $n = 8$; $*p \leq 0.05$; $***p \leq 0.001$ (paired Student's *t* test)

negative as this protein is not part of the exosomal load (middle panel) (Chrobak et al. 2012; Silverman et al. 2010a). We can therefore correlate reduction of infectivity with the lack of Aha1 in immune-modulatory vesicles.

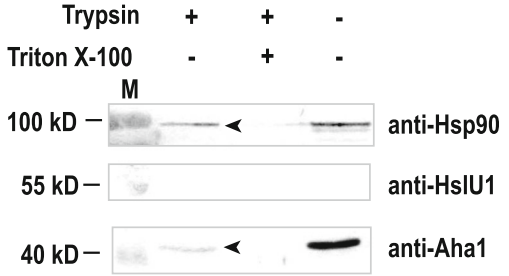

Fig. 8 Detection of Aha1 in the secretome. *L. donovani* wild-type parasites were incubated for 2 h in PBS with 5% sucrose followed by centrifugation, concentration of the cell supernatant and acetone precipitation thereof. The samples were then tested for sensitivity to trypsin in the presence and absence of the detergent Triton X-100. The samples were separated by SDS-PAGE, subjected to Western blot and probed with chicken anti-Hsp90 as a positive control (*upper panel*), mouse anti-HslU1 as a negative control (*middle panel*) and chicken anti-Aha1 (*lower panel*). The *arrowheads* point at Hsp90- and Aha1-specific bands. Positions of size markers [kD] are shown on the *left*

Discussion

The Hsp90 foldosome complexes are essential for function and regulation of a large multitude and variety of client proteins (Buchner 1999; Rutherford and Zuker 1994). To achieve the necessary specificity and coordination of Hsp90 chaperone activity, the Hsp90 complexes can comprise a spectrum of co-chaperones in varying composition (Li et al. 2011, 2012). In addition, the activity of Hsp90 is also subject to regulation by post-translational modifications (Soroka et al. 2012) but also through interaction with certain co-chaperones, e.g. Aha 1 and P23 (Rehn and Buchner 2015).

Although the nature and function of the Hsp90 client proteins in *Leishmania* spp. and related Trypanosomatida are poorly understood to date, nevertheless Hsp90 and its co-chaperones are essential for viability, life cycle control,

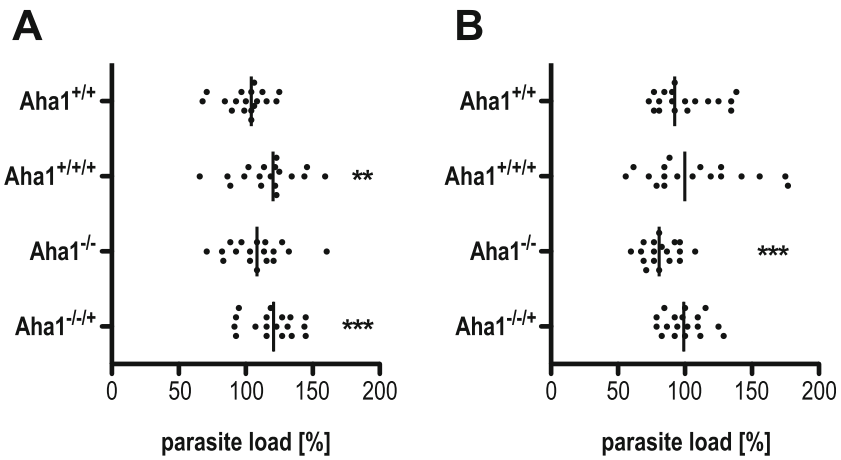

Fig. 7 Effect of Aha1$^{-/-}$ expression on infectivity in vitro. Bone marrow-derived macrophages were infected with *L. donovani* Aha1$^{+/+}$, Aha1$^{+/+/+}$, Aha1$^{-/-}$ and Aha1$^{-/-/+}$ parasites at a ratio of 1:10. After 4 h, free parasites were removed and the infected macrophage cultures were further incubated at 37 °C and 5% CO_2 for 44 h. The gDNAs were isolated after 4.5 h (**a**) and after 48 h (**b**), and subjected to qPCR. The parasite load was calculated as percentage of wild-type parasite load. Six biological replicates, each measured in triplicate ($n = 18$); $**p \leq 0.01$; $***p \leq 0.001$ (paired Student's *t* test)

infectivity and stress tolerance of these important pathogens (Clos and Hombach 2015; Hombach et al. 2013; Morales et al. 2010; Ommen et al. 2010; Vergnes et al. 2007; Wiesgigl and Clos 2001) and, as such, possible targets for therapeutic intervention. Therefore, modulation of Hsp90 activity may have a strong effect on the parasite's overall survivability. After studying the P23 co-chaperone (Hombach et al. 2015), the next logical step therefore was to investigate its presumed antagonist, Aha1.

Previous studies (Rosenzweig et al. 2008; Seraphim et al. 2013) showed that *Leishmania* Aha1 is not a heat-inducible protein. We could confirm this in our experiments. In addition, Aha1 abundance does not fluctuate during a full, 10-day in vitro life cycle (Fig. 1). Seraphim et al. (2013) observed an interaction of recombinant *L. braziliensis* Aha1 and Hsp90 by ITC. Our pull-down analysis of 3HA::Hsp90 and endogenously coded Aha1 failed probably due to the N-terminal localisation of the HA-tag interfering with the interaction of these two proteins (Fig. 2). By contrast, the overexpressed 3HA::Aha1 forms cross-linkable complexes with endogenously coded Hsp90 (Fig. 2). As expected, *L. donovani* Aha1 and Hsp90 are part of the cytosolic fraction according to a fractionation assay (Fig. 3). Unfortunately, a co-staining of Aha1 and Hsp90 and the visualisation by immunofluorescence microscopy was not possible due to unspecific binding of the anti-Aha1 antibody. The results confirm that *Leishmania* Aha1 behaves similarly to other known Aha1 orthologues (Chua et al. 2012; Panaretou et al. 2002; Singh et al. 2014). Whether *Leishmania* Aha1 has interaction partners other than Hsp90 or chaperone activity by itself as described for human Aha1 (Tripathi et al. 2014) remains to be investigated.

The folding and activation of a variety of Hsp90 clients depends on the composition of the foldosome complex, the rate of ATPase turnover and post-translational modifications of Hsp90 itself and of its co-chaperones in an organism-specific manner (Johnson and Brown 2009; Li et al. 2012; Mollapour and Neckers 2012). In *Leishmania* spp., the main players of the foldosome complex are present (Stip1, Cyp40, Sgt, P23, Aha1) while the co-chaperone Cdc37, known to deliver client kinases to the Hsp90 dimer in various eukaryotes, is missing. Concerning post-translational modifications, a phosphoproteome analysis showed Hsp90, Hsp70 and Stip1 to be phosphorylated in a stage-dependent manner (Morales et al. 2010). The *L. braziliensis* Hsp90 ATPase activity, analysed in vitro, was compared to that of other organisms (Silva et al. 2013). This indicates a comparable range of modulatory mechanisms affecting *Leishmania* Hsp90.

The lack of Aha1 in *L. donovani* has no overt growth phenotype under standard cultivation conditions, at elevated temperature or in acidic milieu (Fig. 5). This result is in contrast to results obtained from yeast (Lotz et al. 2003; Panaretou et al. 2002) or *Neurospora crassa* (Gu et al. 2016) regarding temperature sensitivity. A possible explanation for the redundancy of Aha1 function is the low intrinsic ATPase activity of Hsp90 under physiological conditions (Silva et al. 2013). Another possibility is the ability of *Leishmania* to amplify genes and chromosomal regions spontaneously (Rogers et al. 2011; Ubeda et al. 2014), allowing for the possibility that the surviving Aha1$^{-/-}$ parasites have already been selected for a spontaneous genetic complementation.

One effect of the Aha1 loss of function was an increased sensitivity to ethanol (Fig. 5d). In addition to damaging proteins similar to a heat stress, exposure to ethanol affects the plasma membranes of cells and alters the proton transport across them (Cartwright et al. 1986). Apparently, Aha1 plays a role in protecting membrane functionality against ethanol stress by activating Hsp90 folding capacity. It should also be noted that ethanol stress can trigger promastigote-to-amastigote differentiation in *L. donovani* (Barak et al. 2005). In the light of our results, that effect may be due to a disturbance of the Hsp90-co-chaperone homeostasis.

The structurally unrelated Hsp90-specific inhibitors geldanamycin and radicicol are known to compete with ATP for the ATP-binding pocket located at the N-terminus of Hsp90. The binding properties of GA and RAD differ concerning their orientation in the ATP-binding pocket (Roe et al. 1999).

The lack of P23, the supposed antagonist of Aha1, leads to an increased sensitivity against both RAD and GA, in yeast and in *Leishmania* (Forafonov et al. 2008; Hombach et al. 2015). Under RAD treatment, we observed for Aha1 that the overexpression renders the cells sensitive to the inhibitor (Fig. 6a). One possible explanation is that the overexpression of Aha1 results in a hyperstimulation of the ATPase activity leading to a better accessibility and stronger binding of RAD. The putative antagonist of Aha1, P23, inhibits Hsp90 ATPase activity. *L. donovani* P23$^{-/-}$ null mutants show a phenotype similar to Aha1$^{+/+/+}$. The lack of P23 may increase the ATPase activity of Hsp90 leading to a RAD-sensitive phenotype. In contrast, Aha1$^{-/-}$ and P23$^{+/+/+}$ behave like wild-type cells, possibly by decelerating Hsp90 ATPase activity and reducing RAD accessibility. The overexpression of both co-chaperones, Aha1 and P23, have a synergistic growth effect under RAD treatment, supporting our hypothesis that the balance of activation and inhibition of Hsp90 ATPase activity is crucial for protection against RAD binding. Our conclusion will have to be verified by the determination of the Hsp90 ATPase activity within the recombinant *L. donovani* strains.

The common knowledge of the Hsp90 inhibitors GA and RAD suggests a similar functionality with different binding characteristics (Roe et al. 1999). As against that, the effects of RAD on Aha1 expression could not be observed under GA inhibition of Hsp90 (Fig. 6b). Here, Aha1 overexpression causes a wild type-like growth under GA challenge while the Aha1$^{-/-}$ null mutant shows poor GA tolerance. Similar observations were made when testing human Aha1 knockdown cells under the GA derivative 17-AAG. However, no

testing of RAD sensitivity was performed in that study (Holmes et al. 2008). Under GA treatment, Aha1 and P23 null mutants behave similarly. Also, overexpression of both Aha1 and P23 had the same effect under GA inhibition. Here, the combined overexpression of Aha1 and P23 also has an additive effect on GA resistance, possibly by interfering with GA binding to the Hsp90 ATP-binding pocket.

These results suggest that differences in the binding of the two classes of Hsp90 inhibitors are reflected in the opposing effects of Aha1 expression levels. Possible explanations are (i) a change in the ATPase activity of Hsp90 increasing inhibitor susceptibility or (ii) a protective effect against inhibitor binding by co-chaperone overexpression. These explanations need to be substantiated by future experiments.

To analyse the proliferation of intracellular amastigotes of Aha1$^{-/-}$ null mutants, mouse bone marrow-derived macrophages were infected. While the P23 null mutant (Hombach et al. 2015) showed no adverse effects during the intracellular amastigote stage, the Aha1$^{-/-}$ replacement mutant displayed a significant reduction of parasite load. The null mutant infects macrophages in vitro with 80% efficiency compared with the wild type (Fig. 7b). Also, overexpression of Aha1, either before wild type or Aha1$^{-/-}$ background, causes a significantly increased parasite load in the macrophages immediately after infection (Fig. 7a). In the last years, a number of virulence-affecting proteins could be detected in *Leishmania* exosome-like vesicles, such as heat shock protein 100 (Silverman et al. 2010b), *L. major* P46 (Bifeld et al. 2015), cyclophilin 40 (Yau et al. 2016) and antimony resistance marker 56 (Tejera Nevado et al. 2016). Exosomes with their protein payload can attenuate the anti-parasitic properties of host cells and host organisms, thereby furthering their survival and proliferation inside their hosts (Bifeld et al. 2015; Silverman et al. 2010b). The lack of Aha1 in exosomes from null mutants may therefore be the reason for their reduced survival in macrophages.

The earlier work on exosomes missed the presence of Aha1, probably due to the lack of Aha1-specific antibodies. The abundance of Aha1 may be too low for detection by mass spectrometry. It is also noteworthy that most exosome payload proteins are normally cytosolic (Silverman et al. 2008, 2010a). So is Aha1, both in *Leishmania* (Fig. 3a) and in other eukaryotes (Rehn and Buchner 2015). As such, and due to its association with Hsp90, the presence of Aha1 in exosomes (Fig. 8) comes as no surprise since Hsp90-Aha1 complexes have been shown before to be secreted by human cells via exosomes (Ghosh et al. 2015; Park et al. 2010).

In summary, *L. donovani* Aha1 is a functional equivalent to the previously described activator of the Hsp90 ATPase family. It has little impact on general viability, but interferes with the activity of Hsp90 inhibitors. It is part of the exosome-dependent secretome and as such directed to the host cell's cytosol where its activity may modulate the macrophage's defence mechanisms in a pro-parasitic direction.

Acknowledgements We thank Eugenia Bifeld and Julia Eick for providing bone marrow-derived macrophages. The work described here was funded by the Deutsche Forschungsgemeinschaft, Grant CL 120/8-1.

References

Barak E, Amin-Spector S, Gerliak E, Goyard S, Holland N, Zilberstein D (2005) Differentiation of *Leishmania donovani* in host-free system: analysis of signal perception and response. Mol Biochem Parasitol 141:99–108

Bates PA (1993) Axenic amastigote culture of *Leishmania* amastigotes. Parasitol Today 9:143–146

Bates PA (1994) Complete developmental cycle of *Leishmania mexicana* in axenic culture. Parasitology 108:1–9

Batista FA, Almeida GS, Seraphim TV, Silva KP, Murta SM, Barbosa LR, Borges JC (2015) Identification of two p23 co-chaperone isoforms in *Leishmania braziliensis* exhibiting similar structures and Hsp90 interaction properties despite divergent stabilities. FEBS J 282:388–406

Bifeld E, Chrobak M, Zander D, Schleicher U, Schönian G, Clos J (2015) Geographical sequence variation in the *Leishmania major* virulence factor P46. Infect Genet Evol 30:195–205

Bifeld E, Tejera Nevado P, Bartsch J, Eick J, Clos J (2016) A versatile qPCR assay to quantify trypanosomatidic infections of host cells and tissues. Med Microbiol Immunol 205:449–458

Brandau S, Dresel A, Clos J (1995) High constitutive levels of heat-shock proteins in human-pathogenic parasites of the genus *Leishmania*. Biochem J 310(Pt 1):225–232

Buchner J (1999) Hsp90 & Co.—a holding for folding. Trends Biochem Sci 24:136–141

Cartwright CP, Juroszek JR, Beavan MJ, Ruby FMS, Demorais SMF, Rose AH (1986) Ethanol dissipates the proton-motive force across the plasma-membrane of *Saccharomyces cerevisiae*. J Gen Microbiol 132:369–377

Choudhury K, Zander D, Kube M, Reinhardt R, Clos J (2008) Identification of a *Leishmania infantum* gene mediating resistance to miltefosine and SbIII. Int J Parasitol 38:1411–1423

Chrobak M, Förster S, Meisel S, Pfefferkorn R, Förster F, Clos J (2012) *Leishmania donovani* HslV does not interact stably with HslU proteins. Int J Parasitol 42:329–339

Chua CS, Low H, Lehming N, Sim TS (2012) Molecular analysis of *Plasmodium falciparum* co-chaperone Aha1 supports its interaction with and regulation of Hsp90 in the malaria parasite. Int J Biochem Cell Biol 44:233–245

Clos J, Brandau S (1994) pJC20 and pJC40—two high-copy-number vectors for T7 RNA polymerase-dependent expression of recombinant genes in *Escherichia coli*. Prot Expression Purif 5:133–137

Clos, J., and Hombach, A. (2015) Heat shock proteins of *Leishmania*: chaperones in the driver's seat. Leishmania: current biology and control 17–36

Forafonov F, Toogun OA, Grad I, Suslova E, Freeman BC, Picard D (2008) p23/Sba1p protects against Hsp90 inhibitors independently of its intrinsic chaperone activity. Mol Cell Biol 28:3446–3456

Ghosh S, Shinogle HE, Garg G, Vielhauer GA, Holzbeierlein JM, Dobrowsky RT, Blagg BS (2015) Hsp90 C-terminal inhibitors exhibit antimigratory activity by disrupting the Hsp90alpha/Aha1 complex in PC3-MM2 cells. ACS Chem Biol 10:577–590

Gu X, Xue W, Yin Y, Liu H, Li S, Sun X (2016) The Hsp90 co-chaperones Sti1, Aha1, and P23 regulate adaptive responses to antifungal azoles. Front Microbiol 7:1571

Holmes JL, Sharp SY, Hobbs S, Workman P (2008) Silencing of HSP90 cochaperone AHA1 expression decreases client protein activation and increases cellular sensitivity to the HSP90 inhibitor 17-allylamino-17-demethoxygeldanamycin. Cancer Res 68:1187–1196

Hombach A, Ommen G, Chrobak M, Clos J (2013) The Hsp90-Sti1 interaction is critical for *Leishmania donovani* proliferation in both life cycle stages. Cell Microbiol 15:585–600

Hombach A, Ommen G, MacDonald A, Clos J (2014) A small heat shock protein is essential for thermotolerance and intracellular survival of *Leishmania donovani*. J Cell Sci 127:4762–4773

Hombach A, Ommen G, Sattler V, Clos J (2015) *Leishmania donovani* P23 protects parasites against HSP90 inhibitor-mediated growth arrest. Cell Stress Chaperones 20:673–685

Hübel A, Brandau S, Dresel A, Clos J (1995) A member of the ClpB family of stress proteins is expressed during heat shock in *Leishmania* spp. Mol Biochem Parasitol 70:107–118

Johnson JL, Brown C (2009) Plasticity of the Hsp90 chaperone machine in divergent eukaryotic organisms. Cell Stress Chaperones 14:83–94

Kapler GM, Coburn CM, Beverley SM (1990) Stable transfection of the human parasite *Leishmania major* delineates a 30-kilobase region sufficient for extrachromosomal replication and expression. Mol Cell Biol 10:1084–1094

Krobitsch S, Brandau S, Hoyer C, Schmetz C, Hübel A, Clos J (1998) *Leishmania donovani* heat shock protein 100. Characterization and function in amastigote stage differentiation. J Biol Chem 273:6488–6494

Laban A, Wirth DF (1989) Transfection of *Leishmania enriettii* and expression of chloramphenicol acetyltransferase gene. Proc Natl Acad Sci U S A 86:9119–9123

Li J, Richter K, Buchner J (2011) Mixed Hsp90-cochaperone complexes are important for the progression of the reaction cycle. Nat Struct Mol Biol 18:61–66

Li J, Soroka J, Buchner J (2012) The Hsp90 chaperone machinery: conformational dynamics and regulation by co-chaperones. Biochim Biophys Acta 1823:624–635

Lotz GP, Lin H, Harst A, Obermann WM (2003) Aha1 binds to the middle domain of Hsp90, contributes to client protein activation, and stimulates the ATPase activity of the molecular chaperone. J Biol Chem 278:17228–17235

Mann HB, Whitney DR (1947) On a test of whether one of 2 random variables is stochastically larger than the other. Ann Math Stat 18:50–60

Mollapour M, Neckers L (2012) Post-translational modifications of Hsp90 and their contributions to chaperone regulation. Biochim Biophys Acta 1823:648–655

Morales MA, Watanabe R, Dacher M, Chafey P, Osorio y Fortea J, Scott DA, Beverley SM, Ommen G, Clos J, Hem S et al (2010) Phosphoproteome dynamics reveal heat-shock protein complexes specific to the *Leishmania donovani* infectious stage. Proc Natl Acad Sci U S A 107:8381–8386

Ommen G, Clos J (2010) Heat shock proteins in protozoan parasites—*Leishmania* spp. Heat Shock Proteins 4:135–151

Ommen G, Lorenz S, Clos J (2009) One-step generation of double-allele gene replacement mutants in *Leishmania donovani*. Int J Parasitol 39:541–546

Ommen G, Chrobak M, Clos J (2010) The co-chaperone SGT of *Leishmania donovani* is essential for the parasite's viability. Cell Stress Chaperones 15:443–455

Panaretou B, Siligardi G, Meyer P, Maloney A, Sullivan JK, Singh S, Millson SH, Clarke PA, Naaby-Hansen S, Stein R et al (2002) Activation of the ATPase activity of hsp90 by the stress-regulated cochaperone aha1. Mol Cell 10:1307–1318

Park JE, Tan HS, Datta A, Lai RC, Zhang H, Meng W, Lim SK, Sze SK (2010) Hypoxic tumor cell modulates its microenvironment to enhance angiogenic and metastatic potential by secretion of proteins and exosomes. Mol Cell Proteomics 9:1085–1099

Racoosin EL, Beverley SM (1997) *Leishmania major*: promastigotes induce expression of a subset of chemokine genes in murine macrophages. Exp Parasitol 85:283–295

Racoosin EL, Swanson JA (1989) Macrophage colony-stimulating factor (rM-CSF) stimulates pinocytosis in bone marrow-derived macrophages. J Exp Med 170:1635–1648

Rehn AB, Buchner J (2015) p23 and Aha1. Subcell Biochem 78:113–131

Rey-Ladino JA, Joshi PB, Singh B, Gupta R, Reiner NE (1997) *Leishmania major*: molecular cloning, sequencing, and expression of the heat shock protein 60 gene reveals unique carboxy terminal peptide sequences. Exp Parasitol 85:249–263

Roe SM, Prodromou C, O'Brien R, Ladbury JE, Piper PW, Pearl LH (1999) Structural basis for inhibition of the Hsp90 molecular chaperone by the antitumor antibiotics radicicol and geldanamycin. J Med Chem 42:260–266

Rogers MB, Hilley JD, Dickens NJ, Wilkes J, Bates PA, Depledge DP, Harris D, Her Y, Herzyk P, Imamura H et al (2011) Chromosome and gene copy number variation allow major structural change between species and strains of *Leishmania*. Genome Res 21: 2129–2142

Rosenzweig D, Smith D, Opperdoes F, Stern S, Olafson RW, Zilberstein D (2008) Retooling *Leishmania* metabolism: from sand fly gut to human macrophage. FASEB J 22:590–602

Rutherford SL, Zuker CS (1994) Protein folding and the regulation of signaling pathways. Cell 79:1129–1132

Sambrook J, Russell DW (2001) Molecular cloning, 3rd edn. Cold Spring Harbor Laboratory Press, Cold Spring Harbor

Schäfer C, Tejera Nevado P, Zander D, Clos J (2014) ARM58 overexpression reduces intracellular antimony concentration in *Leishmania infantum*. Antimicrob Agents Chemother 58:1565–1574

Schlüter A, Wiesgigl M, Hoyer C, Fleischer S, Klaholz L, Schmetz C, Clos J (2000) Expression and subcellular localization of cpn60 protein family members in *Leishmania donovani*. Biochim Biophys Acta 1491:65–74

Seraphim TV, Alves MM, Silva IM, Gomes FE, Silva KP, Murta SM, Barbosa LR, Borges JC (2013) Low resolution structural studies indicate that the activator of Hsp90 ATPase 1 (Aha1) of *Leishmania braziliensis* has an elongated shape which allows its interaction with both N- and M-domains of Hsp90. PLoS One 8:e66822

Silva KP, Seraphim TV, Borges JC (2013) Structural and functional studies of *Leishmania braziliensis* Hsp90. Biochim Biophys Acta 1834: 351–361

Silverman JM, Chan SK, Robinson DP, Dwyer DM, Nandan D, Foster LJ, Reiner NE (2008) Proteomic analysis of the secretome of *Leishmania donovani*. Genome Biol 9:R35

Silverman JM, Clos J, de'Oliveira CC, Shirvani O, Fang Y, Wang C, Foster LJ, Reiner NE (2010a) An exosome-based secretion pathway is responsible for protein export from *Leishmania* and communication with macrophages. J Cell Sci 123:842–852

Silverman JM, Clos J, Horakova E, Wang AY, Wiesgigl M, Kelly I, Lynn MA, McMaster WR, Foster LJ, Levings MK et al (2010b) *Leishmania* exosomes modulate innate and adaptive immune responses through effects on monocytes and dendritic cells. J Immunol 185:5011–5022

Singh M, Shah V, Tatu U (2014) A novel C-terminal homologue of Aha1 co-chaperone binds to heat shock protein 90 and stimulates its ATPase activity in *Entamoeba histolytica*. J Mol Biol 426:1786–1798

Soroka J, Wandinger SK, Mausbacher N, Schreiber T, Richter K, Daub H, Buchner J (2012) Conformational switching of the molecular chaperone Hsp90 via regulated phosphorylation. Mol Cell 45:517–528

Student (1908) The probable error of a mean. Biometrika 6:1–25

Tejera Nevado P, Bifeld E, Höhn K, Clos J (2016) Clustering of drug resistance and fitness-related genes in *Leishmania infantum*. Antimicrob Agents Chemother 60:5262–5275

Tripathi V, Darnauer S, Hartwig NR, Obermann WM (2014) Aha1 can act as an autonomous chaperone to prevent aggregation of stressed proteins. J Biol Chem 289:36220–36228

Twu O, de Miguel N, Lustig G, Stevens GC, Vashisht AA, Wohlschlegel JA, Johnson PJ (2013) *Trichomonas vaginalis* exosomes deliver cargo to host cells and mediate hostratioparasite interactions. PLoS Pathog 9:e1003482

Ubeda JM, Raymond F, Mukherjee A, Plourde M, Gingras H, Roy G, Lapointe A, Leprohon P, Papadopoulou B, Corbeil J et al (2014) Genome-wide stochastic adaptive DNA amplification at direct and inverted DNA repeats in the parasite *Leishmania*. PLoS Biol 12:e1001868

Vergnes B, Gourbal B, Girard I, Sundar S, Drummelsmith J, Ouellette M (2007) A proteomics screen implicates HSP83 and a small kinetoplastid calpain-related protein in drug resistance in *Leishmania donovani* clinical field isolates by modulating drug-induced programmed cell death. Mol Cell Proteomics 6:88–101

Wandinger SK, Richter K, Buchner J (2008) The Hsp90 chaperone machinery. J Biol Chem 283:18473–18477

Wiesgigl M, Clos J (2001) Heat shock protein 90 homeostasis controls stage differentiation in *Leishmania donovani*. Mol Biol Cell 12: 3307–3316

Yanisch-Perron C, Vieira J, Messing J (1985) Improved M13 phage cloning vectors and host strains: nucleotide sequences of the M13mp18 and pUC19 vectors. Gene 33:103–119

Yau W-L, Pescher P, Macdonald A, Zander D, Retzlaff S, Blisnick T, Rotureau B, Bastin P, Clos J, Späth G (2014) Cyclophilin 40-deficient *Leishmania donovani* fail to undergo stress-induced development of the infectious metacyclic stage. Cell Microbiol 93:80–97

Yau WL, Lambertz U, Colineau L, Pescher P, MacDonald A, Zander D, Retzlaff S, Eick J, Reiner NE, Clos J et al (2016) Phenotypic characterization of a *Leishmania donovani* cyclophilin 40 null mutant. J Eukaryot Microbiol 63:823–833

Zamora-Veyl FB, Kroemer M, Zander D, Clos J (2005) Stage-specific expression of the mitochondrial co-chaperonin of *Leishmania donovani*, CPN10. Kinetoplastid Biol Dis 4:3

Zilberstein D, Shapira M (1994) The role of pH and temperature in the development of *Leishmania* parasites. Annu Rev Microbiol 48:449–470